This article has been accepted for inclusion in a future issue of this journal. Content is final as presented, with the exception of pagination.

Evaluation of Moisture Sorption Characteristics of PV Encapsulants and Edge Sealants Using the Dynamic Vapor Sorption Technique

Suraj Ravindrababu, Harald Becker, Ulrich W. Paetzold, and Paul Gebhardt

***Abstract*—Reliable moisture-diffusion data are vital for assessing photovoltaic (PV) module durability. This work demonstrates dynamic vapor sorption (DVS) as a fast, accurate technique for characterizing the diffusion properties of PV encapsulants and desiccant-filled edge sealants, particularly through direct measurement of the saturation concentration. The measured diffusivity and solubility coefficients for ethylene–vinyl acetate and polyolefin encapsulants agree with published values, while a dual-mode sorption model derived from DVS data predict edge-sealant breakthrough times with a 12% relative error after 8000 h at 85°C/85% RH. Extended to outdoor climates, the model predicts over 25 years of moisture protection for a 2-cm sealant under tropical conditions. The small sample requirement and automated isotherm generation of DVS, together with its limitations, are discussed, highlighting its value for PV material characterization.**

***Index Terms*—Breakthrough time (BTT), dynamic vapor sorption (DVS), degradation, desiccants, edge sealants, ethylene vinyl acetate (EVA), photovoltaic (PV) module, polyolefin (POE), water diffusion.**

I. Introduction

MOISTURE remains a significant degradation stressor in photovoltaic (PV) modules, especially with newer cell technologies [1], [2], [3]. To ensure the reliability of these modules with high-efficiency cells, the design should address factors that inhibit moisture diffusion. An effective way to prevent degradation from moisture is to use low-diffusivity packaging materials, such as polyolefins (POE), thermoplastic polyolefins, polyvinlybutyral, and polyisobutylene (PIB)-based edge sealants, along with a glass–glass configuration [4]. However, modeling moisture diffusion inside a PV module is essential for quantifying reliability. To accurately model the moisture ingress and subsequent failure, the diffusion properties—specifically diffusivity and solubility—must be determined precisely.

In the PV community, several methods have been reported to measure the diffusion characteristics of commercially available PV materials [5]. The most common method uses permeation-based measurement instruments that measures the transient water vapor transmission rate (WVTR) for a thin film of PV module packaging material, as stipulated in IEC 62788-6-2 [6], [7]. Critical diffusion properties, such as diffusivity, solubility, and permeability are derived from WVTR measurements over time [8]. Although this method produces highly sensitive measurements, it is incapable of assessing materials with very low WVTRs [9], like edge sealants. In addition, operational difficulties arise, including leaks and the calibration of sensors in permeation measurement instruments, as noted by Stevens et al. [10]. Nonself-supporting materials, such as edge sealants, must be supported using thin films with high D or porous ceramic supports, which can alter measurement results. Edge sealants are often available in tape form, and if care is not taken when fabricating thin films from them, measurement errors may occur due to the formation of pores or leaks through the material.

Apart from minor issues affecting result accuracy, the major drawback is the inability to measure materials with dual sorption behavior, such as edge sealants with desiccants, which are increasingly used in PV modules [11]. In these materials, an initial transient phase occurs where penetrant water molecules bind to fixed sites, effectively being immobilized [12]. Therefore, the rate of diffusing penetrant is slowed down in comparison to their diffusion in polymer matrix without desiccants. In the case of a sorbate diffusing through the thickness into a thin film of edge sealant with desiccant, the time taken for the sorbate to be first detected at the unexposed surface of the test sample is called the breakthrough time (BTT) [13]. The accurate prediction of BTT in such edge sealants with varying type and composition of desiccant materials is challenging.

The calculation of the BTT for moisture diffusion in edge sealants used in the PV industry has traditionally relied on the Ca film experiment [14], [15]. However, this method is time-consuming, as diffusion in edge sealants occurs very slowly; determining the BTT for high-barrier edge sealants can take several hours [16]. A WVTR measurement of a desiccant-filled PIB-based edge sealant is shown in Fig. 1. The initial transient phase is marked by the blue vertical line, indicating the time

Received 17 April 2026; revised 22 July 2026 and 21 August 2026; accepted 16 September 2026. This work was supported by the German Federal Ministry for Economic Affairs and Energy (BMWE), under Grant 020E-100550326. *(Corresponding author: Paul Gebhardt.)*

Suraj Ravindrababu is with the Fraunhofer Institute for Solar Energy Systems ISE, 79110 Freiburg, Germany, and also with the Karlsruhe Institute of Technology, Light Technology Institute (LTI), 76131 Karlsruhe, Germany.

Harald Becker is with the Kömmerling Chemische Fabrik GmbH, 66954 Pirmasens, Germany.

Ulrich W. Paetzold is with the Karlsruhe Institute of Technology, Light Technology Institute (LTI), 76131 Karlsruhe, Germany.

Paul Gebhardt is with the Fraunhofer Institute for Solar Energy Systems ISE, 79110 Freiburg, Germany (e-mail: paul.gebhardt@ise.fraunhofer.de).

This article has supplementary downloadable material available at https://doi.org/10.1109/JPHOTOV.2026.3736055, provided by the authors.

Digital Object Identifier 10.1109/JPHOTOV.2026.3736055

© 2026 The Authors. This work is licensed under a Creative Commons Attribution 4.0 License. For more information, see https://creativecommons.org/licenses/by/4.0/

This article has been accepted for inclusion in a future issue of this journal. Content is final as presented, with the exception of pagination.

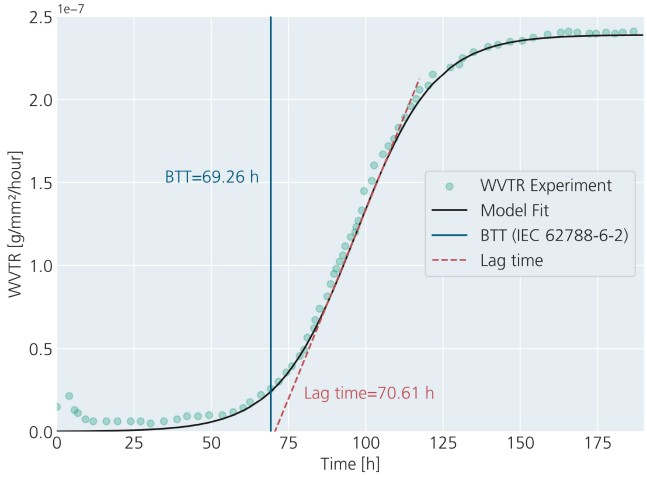


Fig. 1. Typical WVTR measurement of an edge sealant with adsorptive fillers conducted at 85 °C/85% RH. Data are simply fit to a sigmoidal model.

taken for the diffusion process to reach 10% of the steady-state WVTR condition, i.e., BTT according to IEC 62788-6-2. The lag time in the polymer is generally calculated as the intercept of the steady-state portion of the plot on the time axis, represented by the red line [17]. In most contemporary edge sealants, the lag time and BTT are designed to coincide [18]. Although BTT could be deduced from permeation measurements, empirical models, such as Thomas [19] and Yoon [20], have to be used and they require additional information, like the time needed to reach 50% breakthrough and other model constants, necessitating time-consuming tests [21]. Kempe et al. [22] assumed a 3 A desiccant type and modeled moisture absorption in molecular sieves using an empirical model. This method, however, is unusable when the type or composition of molecular sieve is unknown, which is often the case when characterizing commercially available edge sealant materials. In addition, this approach may be unsuitable for developing novel edge sealant materials as moisture barriers for PV applications.

In this article, we introduce the dynamic vapor sorption (DVS) method as a quick, efficient and accurate alternative for characterization of the diffusion properties of commercially available PV materials that allows modeling the BTT of edge sealants with desiccants. Commercially well known POE and ethylene-vinyl acetate (EVA) encapsulants are characterized with the DVS method. Furthermore, a PIB-based edge sealant with desiccant is also characterized using DVS. An analytical model capable of determining the BTT in edge sealants with desiccants is developed by calculating the sorption isotherm of the desiccant from the measurements. The model is validated using experimental results and is extended to predict the BTT outdoors.

II. Experiment

A. Materials

Two commercially available POE and EVA encapsulants, both without ultraviolet blocking additives, were selected for characterization using the DVS technique. For edge sealing analysis, a custom-formulated PIB-based edge sealant, incorporating desiccant and tailored for PV applications, was sourced from a reputable commercial manufacturer.

Encapsulant polymer sheets were cut into 200 mm × 200 mm squares directly from the manufacturer-supplied film rolls. The edge sealant was requested and produced as 100 mm diameter, 1 mm thick circular discs. All cut samples (encapsulants and discs) underwent curing in a Meier vacuum laminator at 150 °C for 10 min, mirroring standard laminate construction settings [23], [24]. Teflon sheets were used to prevent the samples from adhering to the laminator's hot plates. Postcuring thicknesses were measured: the EVA and POE samples were approximately 0.45 and 0.4 mm thick, respectively. The edge sealant sample maintained its original 1 mm thickness. Postfabrication, samples were dried in a climate chamber at 100 °C for 1 h, then sealed in a nitrogen cabinet. For transport to DVS testing, the samples were vacuum-sealed with silica gel to ensure an anhydrous environment.

For validating the BTT of edge sealants, a manual gravimetric test was conducted on samples of edge sealants manufactured at different thicknesses of 2, 6 and 10 mm, respectively. The films were laminated on a stainless steel plate of dimensions 150 mm × 100 mm × 1 mm.

B. Apparatus and Procedure

Tests in this article were conducted using the TA Instruments Q5000 sorption analyzer. The Q5000 SA is a DVS device that produces automated gravimetric measurements of the transient change in sample weight. It uses a microbalance with a sensitivity of 0.1 μg. The system in consideration operates in the temperature range of 0 °C–58 °C and has a relative humidity (RH) control range of 0%–98%.

The device was used in its standard configuration, featuring a reference pan and a quartz sample pan. After sample loading, the humidity chamber was closed and conditioned to the desired temperature and humidity settings. Before the test commences, the sample was dried at the set temperature at 0% RH for 2000 min. The system was programmed to move to the next humidity level when the percentage weight change remained below zero for more than 5 min, indicating the sample had achieved equilibrium. The processed materials were cut into small square-shaped samples with approximate dimensions of 2 mm × 1 mm × sample thickness mm for both the encapsulants and the edge sealant and loaded into the quartz pan [25].

The encapsulants were tested at three temperatures (25 °C, 45 °C, and 58 °C) at five humidity steps (20%, 40%, 60%, 80%, and 85% RH). Regarding the edge sealants, the 25 °C measurement was neglected as it required excessive time to reach saturation. Initial testing of a single sample at a constant temperature of 45 °C showed that the edge sealant requires approximately 4000 min to saturate. To reduce time and costs, the edge sealant was tested at 45 °C and 58 °C at 20%, 60%, and 85% RH. Each test was conducted separately, resulting in six experiments to measure the isotherms at 45 °C and 58 °C. Each experiment was set to run for 4000 min regardless of saturation to avoid

This article has been accepted for inclusion in a future issue of this journal. Content is final as presented, with the exception of pagination.

premature termination of the measurement. Characterizing PIB sealants containing desiccants is challenging, and experimental cutoff times must be determined by trial and error prior to the final measurements.

For the validation experiment through manual gravimetric tests, the samples were kept in a climate chamber at 85 °C and 85% RH and removed periodically to measure the weight of the sample using a microbalance. The weight gain due to moisture is measured using the formula

$$M(\%) = \frac{m_2 - m_1}{m_1 - m_0} * 100\% \tag{1}$$

where m_0 is the mass of the steel plate in g, m_1 is the mass of the plate coated with edge sealant before storage in climate chamber in g, and m_2 is the mass of the plate with edge sealant after storage in climate chamber in g.

III. Theory

This section has two objectives: first, to present the necessary mathematical models and the underlying theory for extracting diffusion properties from DVS measurements; second, to outline the theory and assumptions related to the analytical modeling of BTT for high barrier PV edge sealants based on DVS measurements.

A. Determination of the D and Solubility of Encapsulants

The rate at which an amount of sorbate diffuses in one dimension is given by Fick's second law as stated in (2) [26]. For a thin film that is maintained at a constant sorbate concentration, the amount of diffusing substance, M_t, that has entered the thin film at time t is given by (3), as shown in [27]

$$\frac{\partial C}{\partial t} = D\frac{\partial^2 C}{\partial x^2} \tag{2}$$

$$\frac{M_t}{M_\infty} = 1 - \sum_{n=0}^{\infty} \frac{8}{(2n+1)^2 * \pi^2} exp\left[\frac{-D * (2n+1)^2 * \pi^2 * t}{4 * l^2}\right] \tag{3}$$

where l is the sample half thickness (L) and D is the diffusion constant with physical dimension $L^2\,T^{-1}$. Equation (3) was fitted to the DVS moisture uptake curves, to derive D and M_∞, using a nonlinear least squares algorithm in Python [28].

In thick samples, where the moisture diffusing through the sides cannot be negated, an "edge-effect" correction was done to calculate the actual diffusion constant through [29]

$$D_{\text{corrected}} = D * \left[1 + \frac{l}{w} + \frac{l}{m}\right]^{-2} \tag{4}$$

where w and m are the sample width and breadth, respectively. The concentration of water was derived from M_∞ by dividing it by the sample volume. By calculating the same at different temperatures, the solubility coefficient could be calculated according to Henry's law given as follows:

$$C = S * p_{\text{act}}. \tag{5}$$

Here, p_{act} is the water vapor pressure. The value of p_{act} is determined from the saturation water vapor pressure, p_{sat}, at a given temperature as follows:

$$p_{\text{act}} = \frac{\text{RH}}{100} * p_{\text{sat}}. \tag{6}$$

The value of p_{sat} is determined from the Arden–Buck equation [30]. This calculation is imperative for simulating the ingress of moisture in PV materials exposed outdoors [31]. The temperature variation of the diffusivity and solubility was previously empirically modeled using the Arrhenius Equation [32], given as follows:

$$A = A_0 \exp\left(\frac{-E_a}{k * T}\right) \tag{7}$$

where A is either solubility or diffusivity, A_0 is a pre-exponential factor that has the same unit as A. The term E_a has the unit eV, and when modeling diffusion coefficients, it is called the activation energy of diffusion. When defining the solubility, it is replaced by ΔH_{sol}, which is defined as the heat of solution of penetrant, with the unit eV. The term k is the Boltzmann constant in eV/K, and T is the temperature of the material in Kelvin.

B. Analytical Model for BTT for Edge Sealant With Desiccant

The fundamental model for BTT calculation is derived from Michaels et al. [33] who modeled diffusion in glassy polymers. The diffusion front is represented by two simultaneous processes: the first involves water diffusing through the PIB matrix, which is assumed to follow Henry's sorption law. The second pertains to immobilization sites or pores where water molecules are trapped, following a Langmuir sorption law. Vieth et al. [34] reports this as the "dual sorption" theory. They derived the mathematical form by combining these two distinct sorption behaviors and validated the model for CO_2 sorption in polyester films at a constant temperature [35]. Moreover, they suggest that the isotherm may apply to polymers exhibiting similar behaviors involving two simultaneous sorption mechanisms.

The authors in [36] and [37] extended this theory to calculate the time lag in glassy polymers and in polymers with adsorptive fillers. They demonstrated that the time lag could be calculated for silicone rubber containing a molecular sieve 5 A type desiccant with CO_2, CH_4, N_2, He sorbates.

In this article, we adopt the method proposed by Paul [36] to calculate the BTT for the PIB edge sealant with desiccant and H_2O as the diffusing sorbate. This section highlights the key equations from [36] that are essential for calculating the BTT presented in this article.

The combined sorption isotherm for the PIB edge sealant is given as follows:

$$C = C_H + C_L. \tag{8}$$

The term C_H and C_L refers to the sorption isotherm of the PIB matrix material and that of the desiccant. The subscripts H and L refer to the concentration of water in the component showcasing Henry's and Langmuir sorption isotherms. The (8)

This article has been accepted for inclusion in a future issue of this journal. Content is final as presented, with the exception of pagination.

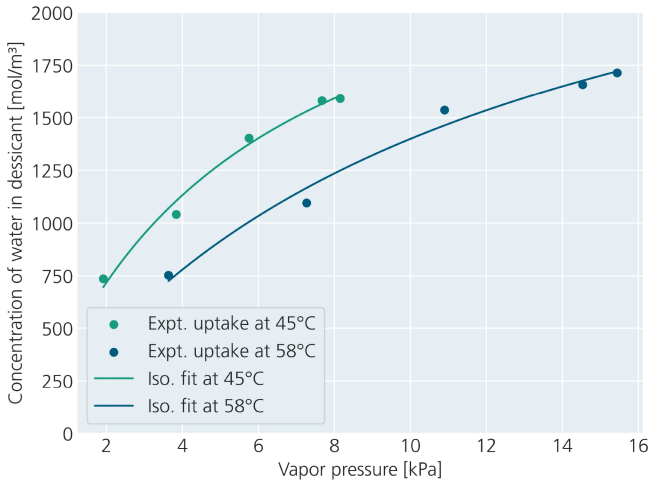


Fig. 2. Sorption isotherm of the desiccant in the edge sealant. Fit using latter half of (9).

could be expanded as follows:

$$C = S * p + \frac{C_A * b * p}{1 + b * p} \tag{9}$$

where S is the solubility of the PIB material without desiccant (pure-PIB) in mol/m^3/kPa, p is the vapor pressure in kPa, C_A is the desiccant saturation constant (mol/m^3), and b is the desiccant affinity constant (kPa^{-1}). The subscript A depicts the concentration of the adsorbed species. Both C_A and b are Langmuir constants.

The parameters that are critical for the calculation of C, i.e., the saturation concentration of the PIB edge sealant in (9), are S, C_A, and b. For the computation of C_A and b, the diffusion characteristics of pure-PIB, i.e., S and C_H have to be determined. If PIB without desiccant is available, S and consequently C_H can be determined by DVS in the same way as described for the encapsulants by assuming that the pure butyl material obeys Henry's law of sorption. The solubility, S of the pure PIB can be obtained by determining the permeability (P) and diffusivity (D) of the pure-PIB material. This leaves only C_A and b to be determined.

C_A and b were obtained by calculating the saturation concentration of the desiccant, i.e., C_L. This was approximated by subtracting C_H from the saturation concentration of the edge sealant measured using DVS. Since the sorption in the desiccant site was assumed to follow a Langmuir isotherm, C_L variation w.r.t vapor pressure was fitted to the latter half of (9), shown in Fig. 2. From this, the values of C_A and b were determined. Since the measurements were conducted for 45 °C and 58 °C at 20%, 60%, and 85% RH, the intermittent values 40% and 80% were obtained through a linear forecast function available in MS Excel to improve the fit. All the four parameters are functions of temperature which were assumed to follow the Arrhenius law and fitted to it empirically.

The permeability (P) of the pure PIB were determined from the steady-state WVTR ($WVTR_{SS}$). These values were provided by the manufacturer of the edge sealant for 23 °C, 38 °C, 60 °C, and 85 °C at 100% RH, measured according to ASTM F1249 [38].

The diffusivity (D) of pure-PIB was determined from values of A_0 (6.12 m^2/hr) and E_a (0.57 eV) reported by Kempe et al. [39]. Using these values, the diffusivity of PIB at 85 °C was determined to be 5.832e-8 m^2/h. In comparison with measurements done by Roosloot et al. [40] on PIB material conducted at 85 °C, which amounts to 6.20833e-8 m^2/h, we find the Arrhenius parameters (A_0 and E_a) determined by Kempe et al. [39] to be usable. The WVTR and $WVTR_{SS}$ can be computed from permeation measurements as follows:

$$\mathrm{WVTR}(t) = \frac{\mathrm{DC}_0}{l}\left(1 + 2\sum_{n=1}^{\infty}(-1)^n.\exp\left(\frac{-D.n^2.\pi^2.t}{l^2}\right)\right)$$

$$\mathrm{WVTR}_{SS} = \frac{\mathrm{DC}_0}{l}. \tag{10}$$

For Fickian materials, the P is the product of diffusion and the solubility coefficient. P can be determined using the available $WVTR_{SS}$ as follows:

$$P = \frac{\mathrm{WVTR}_{SS}.l}{\mathrm{RH} * p_{\mathrm{sat}}} * 100\%. \tag{11}$$

Therefore by computing P and D for PIB at a given temperature and RH combination, S can be determined. Also, the C_H, which is the saturation concentration of PIB [see (8)], is determined from (5).

The solution to the partial differential form of (8) could be derived from the authors in [35] and [36]. Therefore, the time lag (θ), which is equivalent to the BTT of the material is given as follows:

$$\theta = \frac{l^2}{6D}[1 + K * f(y)]$$

$$\text{where}: f(y) = 6y^{-3}\left[\frac{1}{2}y^2 + y - (1+y)ln(1+y)\right] \tag{12}$$

where $y = b * C_{\mathrm{sat}}^{\mathrm{edgesealant}}$, D is the effective sealant diffusion coefficient, $K = \frac{C_A \cdot b}{k_d}$, and k_d is Henry's law coefficient for the pure PIB material $\left(k_d = \frac{P}{D}\right)$.

IV. Results and Discussion

This section discusses the DVS measurements and results derived from the measurements. A comparison is made between DVS measurements and measurements for similar materials available in literature.

A. Discussion on DVS Measurements on Encapsulants

A typical DVS measurement is shown in Fig. 3. With three to four isotherm measurements, the solubility constant of the encapsulants can be determined within 1000 min. This comparably short measurement time, in comparison to permeation or gravimetric methods for realizing complete isotherm profile, demonstrates that DVS is a quick and efficient method. Another significant advantage of such devices is the requirement for small sample sizes, which is particularly useful in situations where a material thin film of sufficient size cannot be produced

This article has been accepted for inclusion in a future issue of this journal. Content is final as presented, with the exception of pagination.

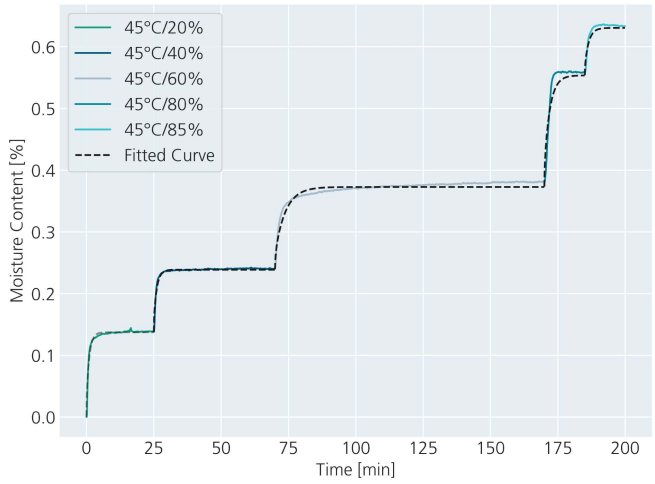


Fig. 3. Typical DVS measurement observed for POE encapsulant at 45 °C. The dotted black line shows the fit with (3) to the measurement data to obtain D and M_∞.

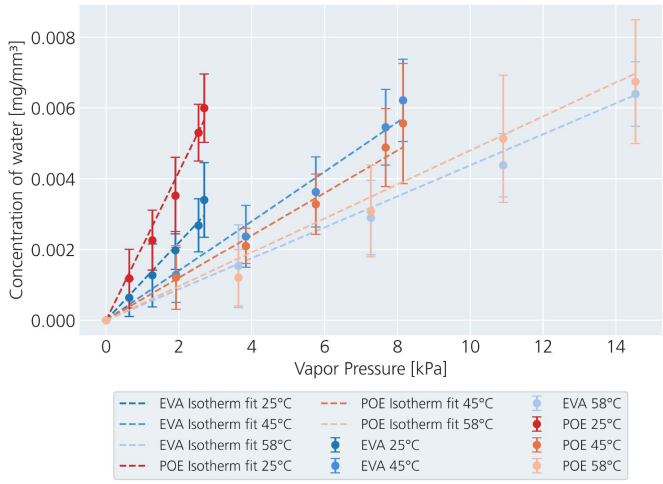


Fig. 4. Sorption isotherms and Henry fits for EVA and POE encapsulant at 25 °C, 45 °C, and 58 °C.

for WVTR measurements. This capability is also beneficial for studying physical changes in polymers that might affect the moisture absorption properties of encapsulants: It is well known that the physical morphology of encapsulants changes during outdoor exposure [41]. In certain studies where encapsulants were exposed to damp-heat conditions, FTIR measurements of EVA showed a nonlinear increase in the hydroxyl index, which is related to water absorption [42].

Consistent with diffusivity coefficients obtained by conventional methods, the coefficients derived from DVS measurements also follow the Arrhenius equation over the investigated range (see supporting information). The critical aspect is the comparison between the diffusivity coefficients determined through model parameters calculated using DVS and the WVTR measurements reported extensively in the literature. For EVA, the reported activation energy for diffusivity coefficient varies from 0.18 eV [7], to 0.45 eV [43]. The activation energy determined by Arrhenius fit to the measured DVS data is 0.41 eV for EVA which fits well within the range stated above. The variation in the diffusion coefficients reported in literature could be caused by several factors, including VA content, curing time, additives etc. [44]. Therefore, it becomes imperative to test for the diffusion properties of the PV module constituents prior to degradation modeling or performance evaluation. DVS serves as an efficient and a quick method in such cases. In the case of POE encapsulants, the comparison of activation energy for diffusion to values from literature is not trivial since it is complicated to identify the correct type of polymer resin. The diffusion coefficient for POE vary in the range of $10^{-10} - 10^{-12}$ m^2/s measured at room temperature. Our model parameters yielded a diffusion coefficient of $1.06e-10$ m^2/s at 25 °C which is closer to the range reported in literature [45].

The solubility coefficients are measured by fitting (5) to the saturation concentration values observed for a sample at prescribed temperature and RH combinations. The Henry isotherm fit for the observed value for EVA and POE encapsulants is shown in Fig. 4. In similar studies reported in the literature,

TABLE I
DIFFUSION AND SOLUBILITY COEFFICIENTS ARRHENIUS MODEL (7) PARAMETERS FOR POE AND EVA ENCAPSULANTS DETERMINED FROM DVS MEASUREMENTS

Encapsulant	Parameter	Values
EVA	$D_0(\mathrm{mm}^2/\mathrm{min})$	36861.63
	$E_a(eV)$	0.41
	$S_0(\mathrm{mol}/m^3/\mathrm{kPa})$	6.17e-8
	ΔH_{sol}	-0.25
POE	$D_0(\mathrm{mm}^2/\mathrm{min})$	509.802
	$E_a(eV)$	0.29
	$S_0(\mathrm{mol}/m^3/\mathrm{kPa})$	5.94e-10
	ΔH_{sol}	-0.38

deviations from Henry's law have been observed [46], [47]. An evaluation of the R^2 values between the experimentally determined concentrations and the corresponding Henry's law fit yielded scores of 0.98 for POE and 0.97 for EVA. As these R^2 values do not indicate a substantial deviation from Henry's model, its application is considered appropriate in this work. The model parameters, including ΔH_{sol}, are listed in Table I were validated by direct comparison with values published by Sidawi et al. [48], who had published similar values for ΔH_{sol} and E_a.

B. Results and Discussion of the BTT Analytical Model

The assumption behind the development of (12) by Vieth et al. [34] and Paul [36] is that the movement of water molecules inside the sealant primarily occurs through the pure butyl material and the desiccant immobilizes the movement of water molecules by trapping them. This assumption has been extended in some articles which predict the BTT of edge sealant material, for example in [22]. Therefore, as appropriately implemented in [37], we consider D to be D_{eff} which is the effective diffusivity of the edge sealant with desiccant rather than PIB. D_{eff} is calculated from the DVS measurements directly by fitting (3) as shown in Fig. 5 for the edge sealant material at 45 °C. A similar treatment to data obtained at 58 °C and fitting (7) to D_{eff} yields A_0 as 7.14e-4 m^2/hr and the activation energy E_a as 0.39 eV. The applicability of (7) for describing the effective D

This article has been accepted for inclusion in a future issue of this journal. Content is final as presented, with the exception of pagination.

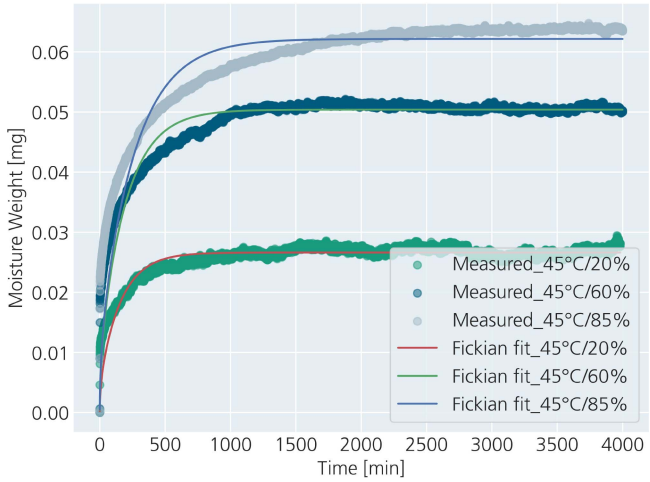


Fig. 5. Moisture uptake of edge sealant measured at 45 °C and at 20%, 60%, and 85% relative humidities. Fit to (3) is shown in the figure.

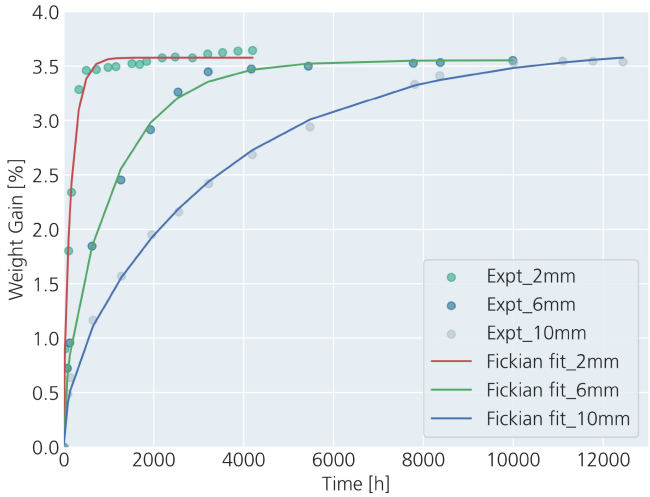


Fig. 6. Moisture uptake for edge sealant BTT validation at different film thicknesses at 85 °C/85%RH. Fit using (3).

TABLE II
CALCULATED ARRHENIUS MODEL PARAMETERS FOR ALL DIFFUSION VARIABLES REQUIRED FOR CALCULATING BTT

Parameter	E_a (eV)	A_0
S^{PIB}, mol/m³/kPa	-0.28	7.57e-4
C_A^{dess}, mol/m³	0.074	39364.6
b^{dess}, kPa^{-1}	-0.5	2.014e-9
$D_{eff}^{\text{PIB+dess}}$, m²/hr	0.39	7.14e-4
D^{PIB}, m²/hr	0.57	6.12
$\text{WVTR}_{\text{SS}}^{\text{PIB}}$, g/m²/d	0.73	2.0825e11

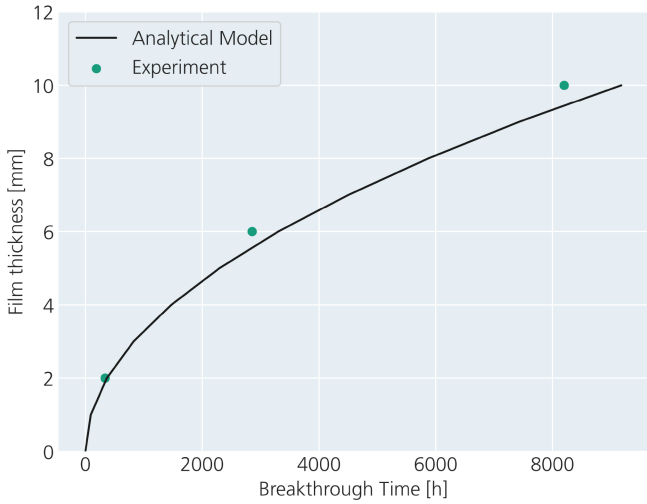


Fig. 7. Comparison of the BTT predictions of the analytical model with experiment at a constant temperature and RH of 85 °C/85% RH. The green dots indicate the BTT calculated from the experiment at 2, 6, and 10 mm thicknesses.

TABLE III
COMPARISON OF BTT BETWEEN EXPERIMENT AND MODEL

Thickness (mm)	BTT Expt / h	BTT Model / h	% rel. error
2	336	367.21	9.29%
6	2856	3304.85	15.72%
10	8200	9180.24	12%

of the edge sealant is validated by comparing the diffusivities obtained from fitting (3) to the manual gravimetric test data in Fig. 6 with those calculated from (7) using the values of A_0 and E_a given above. The data from Fig. 6 yields a diffusivity of $2.42e-9 \pm 2.12e-10$ m^2/h. A_0 and E_a determined from the DVS data give a value of $2.32e-9$ m^2/h, which is very close to the D determined from the manual gravimetric test. However, the applicability of (7) should be verified with moisture uptake experiments. Moisture sorption properties vary hugely depending upon the volume fraction and the type of hydrophilic fillers used in the sealant. Sugiman et al. [49] showcased such differences explicitly, where different volume fractions and fillers showcasing different reactivity to water had a huge impact on the D and the saturation concentration of the material.

The four parameters, C_A, b, D_{eff}, and S, for the pure butyl material are all functions of temperature and were empirically fitted using the Arrhenius law. The corresponding Arrhenius parameters for all diffusion properties required for the calculation of BTT are listed in Table II. Using these values, the BTT under varying field temperature and RH conditions can be predicted, as shown in the next section.

The results of the validation experiment conducted at 85 °C and 85% RH in a climate chamber for the edge sealant material is shown in Fig. 6. The advantage of using DVS for material development and characterization becomes evident when comparing the moisture saturation time required by the conventional gravimetric method and the DVS method. The time taken for saturation of the film is taken as the BTT at that particular thickness. The trend of BTT computed using the analytical model shown here is compared with the experimentally obtained saturation times as shown in Fig. 7. The relative error with respect to the experimentally obtained BTT is shown in Table III. The BTT predicted by the analytical model is only 15% higher than the experimentally measured BTT, even at longer moisture exposure times. Considering the complex diffusion process of a material

This article has been accepted for inclusion in a future issue of this journal. Content is final as presented, with the exception of pagination.

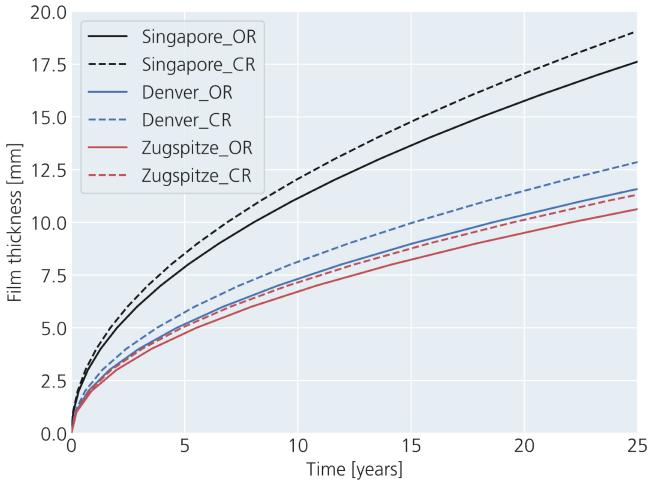


Fig. 8. Comparison of the BTT predictions at different locations and mounting configurations.

containing additives and exhibiting dual sorption behavior with an unknown isotherm, this seems acceptable for an analytical model. The error could be further reduced by measuring even at smaller RH intervals as tested here, which would affect the fitting parameters C_A and b. Furthermore, D_{eff} affects the shift of the curve in Fig. 7. The D_{eff} computed using the measurements at 45 °C and 58 °C, when extrapolated using the Arrhenius model seem to be smaller than the values calculated from the film experiments for validation at 85 °C. This could be an effect of the sample size during our DVS experiments. The smaller surface to volume ratio of the samples in the DVS measurements could also contribute to measurement errors since D_{eff} largely influences the BTT prediction. The volatility in sample size considerations, along with other implications of the measurement steps, such as predrying the sample at 0% RH and the testing temperature before loading it into the DVS instrument, is provided in [50], particularly for hygroscopic moisture barrier materials. Some articles report the sample to be hung by a nonabsorbing metal wire [51]. Future studies should focus on the effects of such sample arrangements on hygroscopic materials.

C. Calculation of BTT in an Outdoor Environment

As previously mentioned, the critical parameters for BTT prediction, D_{eff}, S, C_A, and b, can be determined for varying temperature and RH conditions using the values listed in Table II. In this work, BTT is predicted under outdoor conditions over a period of 25 years for three locations with different climatic conditions. The critical assessment is to understand the influence of temperature and relative humidities at actual geographical locations and module microclimatic conditions. Three locations: Singapore (tropical warm and humid climate), Denver CO (cold and less humid) and Zugspitze in Germany (cold and humid climate). The module temperature was calculated using the King's model as it provides the ability to test for variation of BTT w.r.t mounting configurations [closed rack (CR) and open rack] for glass-glass modules. The predictions are shown in Fig. 8 and

TABLE IV
CALCULATED AVERAGE MODULE TEMPERATURE FOR DIFFERENT MOUNTING CONFIGURATIONS AND AMBIENT RH

Location	Module T CR (K)	Module T OR (K)	RH (%)
Singapore	308.96	305.4	81.6
Zugspitze	287.23	284.9	78.7
Denver	291.92	287.92	52.7

the average calculated module temperature and ambient RH are shown in Table IV.

From Fig. 8, it is apparent that temperature plays a greater role in the determination of BTT. This is unsurprising since the role of RH affects only S, i.e., the amount of water absorbed by the PIB phase when exposed to the environment. The diffusion inside the edge sealant, mainly controlled by D_{eff}, is a function of the temperature. It is important to note that as temperature becomes colder, the effect of mounting configurations reduce. This is due to the parameter configuration in the King's model and its effect on the module temperature. From Table IV, it can be seen that the module temperature difference between open and CR configurations become smaller as the temperature becomes colder. The observation of models' impact on predicting PV material behavior in outdoor environments underscores the necessity for ongoing development of advanced models that accurately forecast the dynamic variations in environmental loads on PV modules.

V. CONCLUSION

In this study, we demonstrated that DVS is a viable, accurate, and quick method for measuring the diffusion properties of encapsulants and high-moisture-barrier edge sealant materials with desiccants. The validity of DVS as a method for measuring the diffusion properties of PV materials is demonstrated by testing two encapsulants, EVA and POE, as well as an edge sealant containing a desiccant. The calculated diffusion properties are compared in detail with those reported in the literature using conventional methods, such as gravimetric and permeation measurements. The presented model predicts the BTT for edge sealants, achieving a relative error of 12% after prolonged exposure times exceeding 8000 h at a constant temperature and RH of 85 °C and 85% RH. Our validated model shows that the high moisture barrier material takes more than 25 years to penetrate through 2 cm thick edge sealant material exposed to a tropical hot and humid environment, such as Singapore.

The most critical advantage of DVS is its small sample size requirement and the automated generation of complete isotherms. These features are particularly important for predicting reliability, as literature indicates varying diffusion capacities of PV materials due to changes in their physical morphology during outdoor exposure. In addition, materials exhibiting different types of isotherms can also be analyzed. These advantages underscore the potential of DVS as a valuable tool for characterizing PV materials.

It is important to note that the experimental DVS settings for measuring high-barrier materials and encapsulants differ. This is primarily due to the long saturation time required for

This article has been accepted for inclusion in a future issue of this journal. Content is final as presented, with the exception of pagination.

high-barrier materials. In addition, the experimental cutoff times for high-moisture-barrier materials must be established to ensure sample saturation. This can be cumbersome, particularly when the effect of the desiccant and its volume fraction is significant, i.e., when the saturation concentration of desiccants is high, which is often the case for high-performance materials. Clarity on the effects of sample size, weight, and the necessity of predrying steps during DVS measurements should also be investigated, especially when analyzing hygroscopic materials. Another limitation of DVS is its inability to measure PV materials with multiple layers, such as backsheets. To be absorbed into the module and diffuse through the encapsulant, moisture must first penetrate all layers of the backsheet. However, the diffusion properties of the different layers typically vary for most backsheets. This complicates the calculation of transient diffusion. However, if the multilayer constituents are available individually, DVS measurements of the individual components could be employed to determine the transient diffusion in multilayered materials, as demonstrated by Zhang et al. [52]. Future work could involve quantifying uncertainty in DVS measurements of PV material samples and assessing how measurement uncertainties affect the modeling of degradation in PV systems.

Acknowledgment

The authors would like to thank Dr. Carolin Schmidt and Dr. Harald Rohm at the Institute of Natural Materials Technology at TU Dresden for conducting measurements using the TA Q5000SA device.

References

[1] Y. Wang et al., "Encapsulation and stability testing of perovskite solar cells for real life applications," *ACS Mater. Au*, vol. 2, no. 3, pp. 215–236, 2022.

[2] K. Yan et al., "Causes of moisture-induced corrosion around n-topcon photovoltaic modules and pre-study of high-reliability packaging solutions," *Renewable Energy*, vol. 248, 2025, Art. no. 123148.

[3] P. Gebhardt, U. Kräling, E. Fokuhl, I. Hädrich, and D. Philipp, "Reliability of commercial topcon PV modules—An extensive comparative study," *Prog. Photovolt.: Res. Appl.*, vol. 33, no. 12, pp. 1378–1386, 2025.

[4] A. K. Öz et al., "Pushing the boundaries: Challenges that arise in manufacturing and designing photovoltaic modules for new application areas," *Sol. Energy Mater. Sol. Cells*, vol. 291, 2025, Art. no. 113735.

[5] O. K. Segbefia, A. G. Imenes, and T. O. Saetre, "Moisture ingress in photovoltaic modules: A review," *Sol. Energy*, vol. 224, pp. 889–906, 2021.

[6] International Electrotechnical Commission, "Measurement procedures for materials used in photovoltaic modules - Part 6-2: General tests - Moisture permeation testing of polymeric materials," *Int. Electrotechnical Commission*, Geneva, CH, Standard, Mar. 2020. [Online]. Available: https://webstore.iec.ch

[7] N. Kim and C. Han, "Experimental characterization and simulation of water vapor diffusion through various encapsulants used in PV modules," *Sol. Energy Mater. Sol. Cells*, vol. 116, pp. 68–75, 2013.

[8] N. Roosloot, D. Lindholm, J. H. Selj, and G. Otnes, "Gravimetric analysis of edge sealant moisture protection in a floating photovoltaic application," *IEEE J. Photovolt.*, vol. 15, no. 3, pp. 442–450, May 2025.

[9] K. L. Jarvis et al., "Comparing three techniques to determine the water vapour transmission rates of polymers and barrier films," *Surfaces Interfaces*, vol. 9, pp. 182–188, 2017.

[10] M. Stevens, S. Tuomela, and D. Mayer, "Water vapor permeation testing of ultra-barriers: Limitations of current methods and advancements resulting in increased sensitivity," in *Proc. Soc. Vac. Coaters 48 th Annu. Tech. Conf. Proc.*, 2005, pp. 189–191.

[11] M. D. Kempe, A. Watts, T. Shimpi, S. Ellis, and K. Barth, "Modeling of the effectiveness of novel edge seal designs for fast, low-capex manufacturing," *Energy Sci. Eng.*, vol. 11, no. 7, pp. 2314–2329, 2023.

[12] C. Most Jr, "Some filler effects on diffusion in silicone rubber," *J. Appl. Polym. Sci.*, vol. 14, no. 4, pp. 1019–1024, 1970.

[13] D. H. Anna, E. T. Zellers, and R. Sulewski, "ASTM F739 method for testing the permeation resistance of protective clothing materials: Critical analysis with proposed changes in procedure and test-cell design," *Amer. Ind. Hyg. Assoc. J.*, vol. 59, no. 8, pp. 547–556, 1998.

[14] M. D. Kempe, A. A. Dameron, and M. O. Reese, "Calcium based test method for evaluation of photovoltaic edge-seal materials (presentation)," *Nat. Renewable Energy Lab., Golden, CO*, Feb. 2011. [Online]. Available: https://docs.nlr.gov/docs/fy11osti/50839.pdf.

[15] M. D. Kempe, A. A. Dameron, and M. O. Reese, "Evaluation of moisture ingress from the perimeter of photovoltaic modules," *Prog. Photovolt.: Res. Appl.*, vol. 22, no. 11, pp. 1159–1171, 2014.

[16] M. D. Kempe, A. A. Dameron, T. J. Moricone, and M. O. Reese, "Evaluation and modeling of edge-seal materials for photovoltaic applications," in *Proc. 35th IEEE Photovolt. Specialists Conf.*, 2010, pp. 00256–00261.

[17] C.-C. Kao, S.-C. Chen, and M.-T. Sheu, "Lag time method to delay drug release to various sites in the gastrointestinal tract," *J. Controlled Release*, vol. 44, no. 2–3, pp. 263–270, 1997.

[18] A. Bonucci et al., "Thin-film CIGS PV modules with more than 3000 h damp heat stability: Breakthrough time property of the B-dry edge sealant and its characterization," *Sol. Energy Mater. Sol. Cells*, vol. 98, pp. 398–403, 2012.

[19] H. C. Thomas, "Heterogeneous ion exchange in a flowing system," *J. Amer. Chem. Soc.*, vol. 66, no. 10, pp. 1664–1666, 1944.

[20] Y. H. Yoon, J. H. Nelson, J. Lara, C. Kamel, and D. Fregeau, "A theoretical model for respirator cartridge service life for binary systems: Application to acetone/styrene mixtures," *Amer. Ind. Hyg. Assoc. J.*, vol. 53, no. 8, pp. 493–502, 1992.

[21] H. B. S. Lima et al., "Parameter estimation of breakthrough curve models in the adsorption process of H_2S and CO_2 using the Markov chain Monte Carlo method," *Appl. Sci.*, vol. 14, no. 16, 2024, Art. no. 6956.

[22] M. D. Kempe, D. L. Nobles, L. Postak, and J. A. Calderon, "Moisture ingress prediction in polyisobutylene-based edge seal with molecular sieve desiccant," *Prog. Photovoltaics: Res. Appl.*, vol. 26, no. 2, pp. 93–101, 2018.

[23] C. Peike, S. Hoffmann, I. Dürr, K.-A. Weiß, and M. Koehl, "The influence of laminate design on cell degradation," *Energy Procedia*, vol. 38, pp. 516–522, 2013.

[24] A. K. Öz et al., "The impact of the lamination process on the adhesion properties at the glass-encapsulant interface and damp heat stability of PV modules," in *Proc. 38th Eur. PV Sol. Energy Conf. Exhib.*, 2021, vol. 6, pp. 708–714.

[25] A. Nistor, G. Stiubianu, C. Racles, and M. Cazacu, "Evaluation of the water sorption capacity of some polymeric materials by dynamic vapour sorption," *Mater. Plast*, vol. 48, no. 1, pp. 33–37, 2011.

[26] A. Fick, "Ueber diffusion," *Annalen der Physik*, vol. 170, no. 1, pp. 59–86, 1855. [Online]. Available: https://onlinelibrary.wiley.com/doi/abs/10.1002/andp.18551700105

[27] J. Crank, *The Mathematics of Diffusion*, Oxford Univ. Press, Oxford, U.K, 1979.

[28] P. Virtanen et al., "SciPy 1.0: Fundamental algorithms for scientific computing in Python," *Nature methods*, vol. 17, no. 3, pp. 261–272, 2020.

[29] C.-H. Shen and G. S. Springer, "Moisture absorption and desorption of composite materials," *J. Composite Mater.*, vol. 10, no. 1, pp. 2–20, 1976.

[30] A. L. Buck, "New equations for computing vapor pressure and enhancement factor," *J. Appl. Meteorol. Climatol.*, vol. 20, no. 12, pp. 1527–1532, 1981.

[31] S. Mitterhofer et al., "Measurement and simulation of moisture ingress in PV modules in various climates," *IEEE J. Photovolt.*, vol. 14, no. 1, pp. 140–148, Jan. 2024.

[32] L. W. McKeen, "1 - introduction to permeation of plastics and elastomers," in *Permeability Properties of Plastics and Elastomers*, 3rd ed. ser. Plastics Design Library, L. W. McKeen, Ed., Oxford, U.K.: William Andrew Publishing, 2012, pp. 1–20. [Online]. Available: https://www.sciencedirect.com/science/article/pii/B9781437734690100013

[33] A. S. Michaels, W. R. Vieth, and J. A. Barrie, "Diffusion of gases in polyethylene terephthalate," *J. Appl. Phys.*, vol. 34, no. 1, pp. 13–20, 1963. [Online]. Available: https://doi.org/10.1063/1.1729054

This article has been accepted for inclusion in a future issue of this journal. Content is final as presented, with the exception of pagination.

[34] W. R. Vieth, J. Howell, and J. Hsieh, "Dual sorption theory," *J. Membrane Sci.*, vol. 1, pp. 177–220, 1976.
[35] W. R. Vieth and K. Sladek, "A model for diffusion in a glassy polymer," *J. Colloid Sci.*, vol. 20, no. 9, pp. 1014–1033, 1965.
[36] D. Paul, "Effect of immobilizing adsorption on the diffusion time lag," *J. Polym. Sci. Part A-2: Polym. Phys.*, vol. 7, no. 10, pp. 1811–1818, 1969.
[37] D. Paul and D. Kemp, "The diffusion time lag in polymer membranes containing adsorptive fillers," In J. Polym. Sci.: Polym. Symposia, Vol, vol. 41, no. 1, p.
[38] *ASTM F1249-20: Standard Test Method for Water Vapor Transmission Rate Through Plastic Film and Sheeting Using a Modulated Infrared Sensor*, ASTM International, West Conshohocken, PA, 2020. [Online]. Available: https://www.astm.org
[39] M. D. Kempe, D. Panchagade, M. O. Reese, and A. A. Dameron, "Modeling moisture ingress through polyisobutylene-based edge-seals," *Prog. Photovolt.: Res. Appl.*, vol. 23, no. 5, pp. 570–581, 2015.
[40] N. Roosloot, D. Lindholm, J. H. Selj, and G. Otnes, "Gravimetric analysis of edge sealant moisture protection in a floating photovoltaic application," *IEEE J. Photovolt.*, vol. 15, no. 3, pp. 442–450, May 2025.
[41] G. Oreski and G. M. Wallner, "Damp heat induced physical aging of PV encapsulation materials," in *Proc. 12th IEEE Intersociety Conf. Thermal Thermomechanical Phenomena Electron. Syst.*, 2010, pp. 1–6.
[42] B. Adothu, F. R. Costa, and S. Mallick, "Damp heat resilient thermoplastic polyolefin encapsulant for photovoltaic module encapsulation," *Sol. Energy Mater. Sol. Cells*, vol. 224, 2021, Art. no. 111024.
[43] M. Jankovec et al., "In-situ monitoring of moisture ingress in PV modules using digital humidity sensors," *IEEE J. Photovolt.*, vol. 6, no. 5, pp. 1152–1159, Sep. 2016.
[44] S. Marais, Q. T. Nguyen, D. Langevin, and M. Métayer, "Transport of water and gases through EVA copolymer films, EVA70/PVC, and EVA70/PVC/gluten blends," *Macromol. Symposia*, vol. 175, no. 1, p.
[45] A. Kitagishi, S. Takizawa, Y. Sato, and H. Inomata, "Measurement and prediction of solubilities and diffusion coefficients of ethylene in rubbery propylene copolymers," *Fluid Phase Equilibria*, vol. 492, pp. 110–117, 2019.
[46] R. Meitzner and S.-H. Schulze, "Method for determination of parameters for moisture simulations in photovoltaic modules and laminated glass," *Sol. Energy Mater. Sol. Cells*, vol. 144, pp. 23–28, 2016. [Online]. Available: https://www.sciencedirect.com/science/article/pii/S0927024815004079
[47] N. Kyranaki, "Corrosion in crystalline silicon photovoltaic modules and the influence on performance," Ph.D. dissertation, Loughborough Univ., 2020.
[48] T. Sidawi et al., "Moisture ingress and distribution in bifacial silicon photovoltaics," *IEEE J. Photovolt.*, vol. 13, no. 3, pp. 365–372, May 2023.
[49] S. Sugiman, S. Salman, and M. Maryudi, "Effects of volume fraction on water uptake and tensile properties of epoxy filled with inorganic fillers having different reactivity to water," *Mater. Today Commun.*, vol. 24, 2020, Art. no. 101360.
[50] TA Instruments, "Dynamic vapor sorption sampling considerations," TA Instruments, Application Note TA334, 2007, Accessed: May 22, 2024. [Online]. Available: https://www.tainstruments.com/pdf/literature/TA334\%20DVS\%20Sampling\%20Considerations.pdf
[51] K. Jansen, M. Zhang, L. Ernst, D.-K. Vu, and L. Weiss, "Effect of temperature and humidity on moisture diffusion in an epoxy moulding compound material," *Microelectronics Rel.*, vol. 107, 2020, Art. no. 113596.
[52] S. Zhang, Y. Liu, P. Feng, and P. Prabhakar, "Moisture diffusion in multilayered materials: The role of layer stacking and composition," *Composites Part B: Eng.*, vol. 293, 2025, Art. no. 112128.